INNER WALL ATTACK AND ITS INHIBITION METHOD FOR FBR FUEL PIN CLADDING AT HIGH BURNUP

XA9848045

XU YONGLI, LONG BIN, LI JINGANG, WAN JIAYING
China Institute of Atomic Energy,
Beijing, China

Abstract

The inner wall attack of the modified 316-Ti S.S. cladding tubes manufactured in China used FBR at 10at.% burnup was investigated by means of the out of pile simulation tests. The inner surface morphologies of the cladding tubes attacked by fission products Cs,Te,I and Se at 700℃ under lower and high oxygen potentials were observed respectively, and the depth of attack was also measured. The burst strength, maximum circum expansion and the appearances of fracture were measured and observed respectively for the cladding tubes attacked by fission products. Based on the mechanism of FBR fuel cladding chemical interaction (FCCI), Cr,Zr and Nb were used as the oxygen absorbers respectively, in order to inhibit the inner wall attack of the cladding tubes. The corrosion morphologies and depth, the penetration depth of the fission products in the inner surface of the cladding tubes were detected. The inhibition effectiveness of the oxygen absorbers for the inner wall attack of the cladding tubes was evaluated.

1.INTRODUCTION

A number of the in pile irradiation tests of the oxide fuel pins have indicated that the attack depth of the cladding inner wall caused by fuel cladding chemical interaction (FCCI) at high burnup will exceed greatly the corrosion margin for fuel pin cladding design, the maximum attack depth is nearly 150μm, and there are three kinds of essential attack morphologies on the inner surface of cladding[1-5]. As all know, both descreasing in the thickness and local intergranular attack will degrade the mechanical properties and limit the life time of the cladding tube.Therefore, the inner wall attack and its inhibition method should be given more attention for the FBR fuel pin design used at high burnup.

The purpose of this paper is to describe primarily the inner wall attack characteristics caused by fission products for the modified 316-Ti S.S. cladding tubes manufactured in China, in order to provide the information for in pile irradiation tests of the domestic cladding in the near future and to investigate the possibility of the inhibition of inner wall attack for the fuel pin cladding tubes used at high burnup.

2.EXPERIMENTAL

Three kinds of 316-Ti S.S. tubes Φ6×0.4mm manufactured in China were used as the specimens in this investigation.

Their composition are listed in table 1. The Cr/Cr_2O_3 and Ni/NiO were used as oxygen buffer respectively, to establish the different oxygen potential.

Cs,I,Te and Se mixture was used as the simulation fission products, and their quantities correspond to those generated when the burnup reaches 10at.%[1].

The buffer and Te, I, Se mixture were loaded into the cladding tubes through a Kovar tube,and degased under vacuum. For the specimens used to investigate the inhibition effectiveness of the

TABLE 1 CHEMICAL COMPOSITION OF 316-TI S.S. TUBES (wt.%)

Specimens	Elements											C.W.(%)
	C	Cr	Ni	Mo	Mn	Si	Ti	P	S	B	Fe	
I	0.07	14.97	15.23	1.20	0.73	0.68	0.45	—	—	0.06	balance	15
II	0.04	16.8	12.5	3.17	1.67	0.73	0.63	0.016	0.0078	—	balance	30
III	0.066	17.08	12.75	2.25	1.37	0.67	0.68	0.028	0.016	—	balance	15

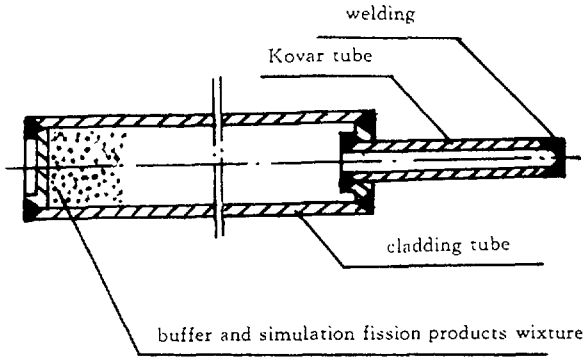

FIG.1 Profile of the prepared cladding tube specimen

inner wall attack, Cr, Zr and Nb powder were loaded respectively into the cladding tubes together with the Ni/NiO buffer and the fission products. Their quantity corresponds to the oxygen absorber coating 25 μ m thick on the surface of the fuel pellet (Φ5.1×high 100mm). Then Cs was injected quantitatively into the cladding tubes by a microinjector in a glove box with high purity inert gas (H_2O<10ppm, O_2<5ppm), the tubes were welded first and afterwards by a cold welding pliers and argon arc for sealing.The prepared specimens (Fig.1) were installed into a capsule with Ar and annealed in a furnace at 700℃ for 120h. The specimens attacked by fission products at lower and high oxyen potentials were connected respectively with a burst machine to measure their burst strength and maximum circum expansion.

3.RESULTS AND DISCUSSION

3.1 Attack characteristics

3.1.1 The attack under lower oxygen potential

The equilibrium oxygen potential established by Cr/Cr_2O_3 at 700℃ is near the level of the oxydation threshold of Cr in stainless steel. Most of the inner surface of 316-Ti cladding tubes have not been attacked by the fission products under this oxygen potential. The shallow intergranular attack (IGA) is observed only at local surface of the specimens (Fig.2). Their maximum IGA depth is less than 28 μ m. EDAX demonstrates that there are no Cs and Te penetration on the inner surface of the cladding tubes.

Thermodynamics investigations of fission produots[1,6,7] indicate that the reactive fission products Cs, I, Te and Se react with each other to some extent and form the stable Cs_2Te, Cs_2Se and CsI at lower oxygen potential. The formation of these cesium compounds makes the attack of single fission products to stainless steel reduce. A little or no reaction occurs between Cr_2O_3 and Cs under this oxygen potential[7].

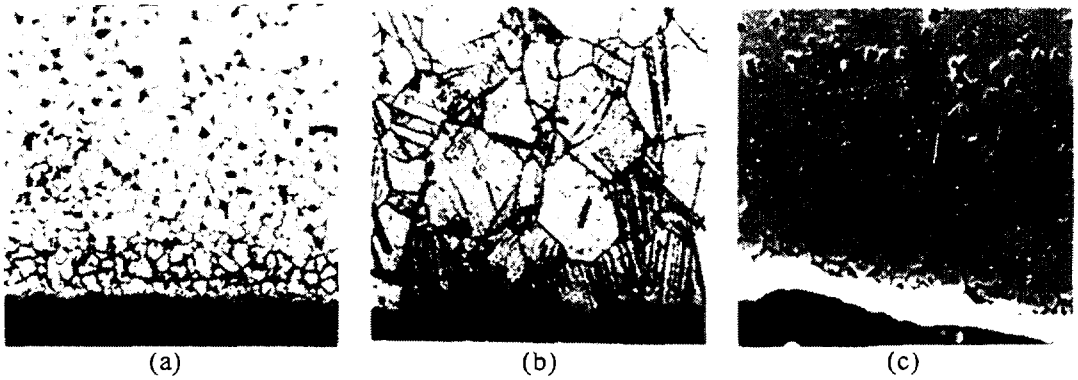

FIG.2 Shallow intergranular attack under lower oxygen potential with Cr/Cr_2O_3
(a)cladding tube I (b)cladding tube II (c)cladding tube III

3.1.2 The attack under high oxygen potential

The matrix erosive attack and IGA occur simultaneously under high oxygen potential established by Ni/NiO buffer. The cladding inner surface appears to be dissolved by fission products, and the grains of matrix are stripped due to IGA and oxidative attack. The attacked zone on local inner surface appears to be "Ulcer" (Fig.3). In this case, the maximum attack depth is about 100 μ m.

Face-scanning indicates that the erosion zone consists of rich Cr/depleted Ni and rich Ni/depleted Cr layers alternatively (Fig.4). EDAX demonstrats that rich Cr is always accompanied by Te and Cs. It can be seen from Fig.5 that the attack depth is approximatly proportional to depletion of Cr, Ni and the penetration depth of Cs and Te in the inner surface of the cladding.

Under high oxygen potential, CsI and the cesium chalcogenides are no longer stable thermodynamically, but cesium chromate become stable[1,6-8]. Therefore, the "Ulcer" erosion may result from the reactions of Cs and Te with cladding. The reactions can be expressed respectively as following[6,7,9]:

$$Cs+Cr_2O_3 \rightarrow Cs_xCrO_4 \quad (x=2,3,4) \qquad (1)$$
$$2xCs+2O_2+FeCr_2O_4 \rightarrow 2Cs_xCrO_4+Fe \qquad (2)$$
$$xCs+Cr+2O_2 \rightarrow Cs_xCrO_4 \qquad (3)$$
$$1/23Cr_{23}C_6+xCs+O_2 \rightarrow Cs_xCrO_4+6/23C \qquad (4)$$
$$6C+23Cr \rightarrow Cr_{23}C_6 \qquad (5)$$

Due to the reaction of Cs with cladding, the partial potential of Cs is reduced and Te activity is increased, the reaction of Te with cladding occurs as[8,10]: $2Cr+3Te \rightarrow Cr_2Te_3$ (6)

(a) (b) (c)

FIG.3 Erosive attack under high oxygen potential with Ni/NiO
(a)cladding tube I (b)cladding tube II (c)cladding tube III

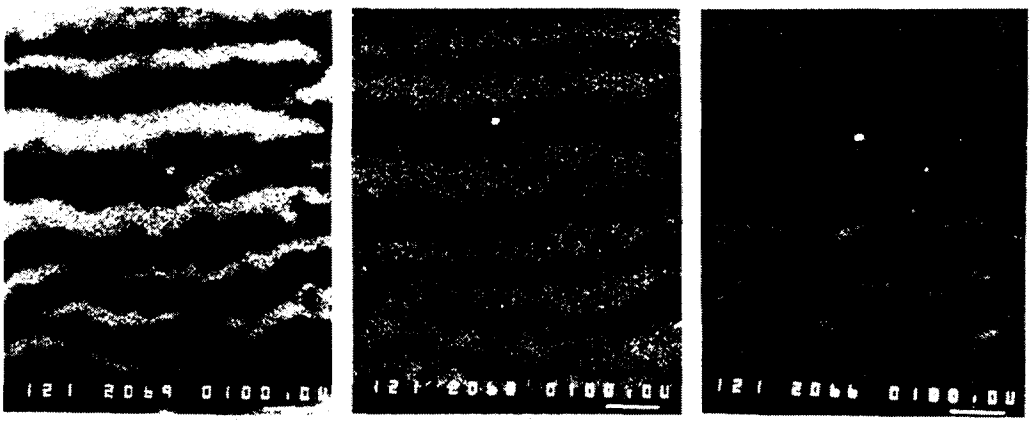

(a) (b) (c)

FIG.4 Distribution of Fe,Ni and Cr in attacked zone
(a)Fe (b)Cr (c)Ni

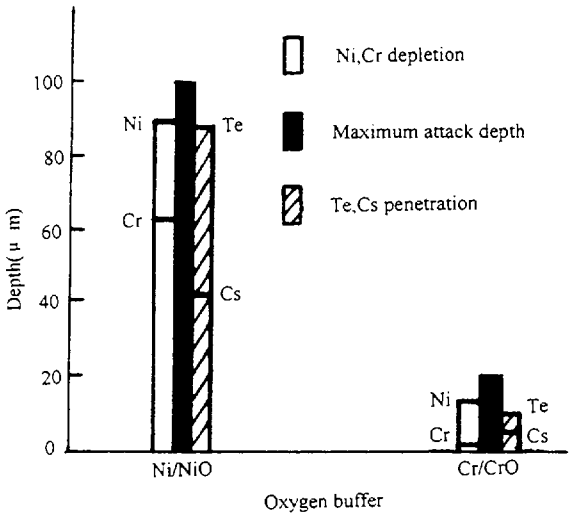

FIG.5 Maximum attack, Te,Cs penetration and Ni,Cr depletion depth

On the other hand, Te and Se penetrate along the grain boundary of cladding, and induce the embrittlement of the grain boundary. When oxygen potential is high enough, cesium chalcogenides react also with the composition elements of cladding as following[8]:

$$Cs_2Te+Cr_2+(Fe,Ni,Cr)O_2 \rightarrow Cs_xCrO_4+(Fe,Ni)Te \quad (7)$$

In this case, the stripping of matrix grain becomes severe.

3.2 Burst strength and circum expansion

Fuel pin cladding suffers the stress due to the internal pressure increasing and the mechanical interaction between cladding and pellets at high burnup. On the other hand, the cladding is also weakened by internal fission products attack. Therefore, it is necessary to understand the mechanical properties change of the cladding after fission products attack. Many tests about this topic have been performed in other countries[11-17]. In this paper, the burst strength and maximum circum expansion of the cladding tubes I and II were measured, the results are shown in table 2 、 Fig.6 and Fig.7.

It can be seen from table 2 that the strength of cladding tube II is degradated and his circum expansion is improved at lower oxygen potential as compared with those of cold work tubes. It may result mainly from annealing effect. Comparing with those of annealing tubes, the burst strength of attacked cladding tubes seems to be no many change, and their circum expansion are slightly low. For cladding tube I attacked under lower oxygen potential, the strength and circum expansion are degraded slightly. The burst strength and circum expansion have not been obtained for the cladding tubes attacked under high oxygen potential, because they breacked down before the measurements were completed.

The appearances of fracture for the cladding tubes I and II attacked under lower and high oxygen potentials are shown in Fig.6. It can be seen that the appearance of fracture is intergranular brittle for the attacked cladding tubes under high oxygen potential, while the tenacious is for those of the annealing and lower oxygen potential.

The axial sections of the bursted cladding tubes are shown in Fig.7. The bursted cladding tubes are shown in Fig.8.

The inner surface is nearly no change for the cladding tubes attacked under lower oxygen potential, the stripping of matrix grain caused by IGA is for those attacked under high oxygen potential. It is clear that the grain boundaries embrittlement is resulted from the fission products attack under high oxygen potential.The Cs and Te penetration in the brocken grain boundaries which is shown in Fig.5 is another evidence for this.This phenomen may be the liguid metal embrittlement which has been described in many papers[10,13,14,18.19].

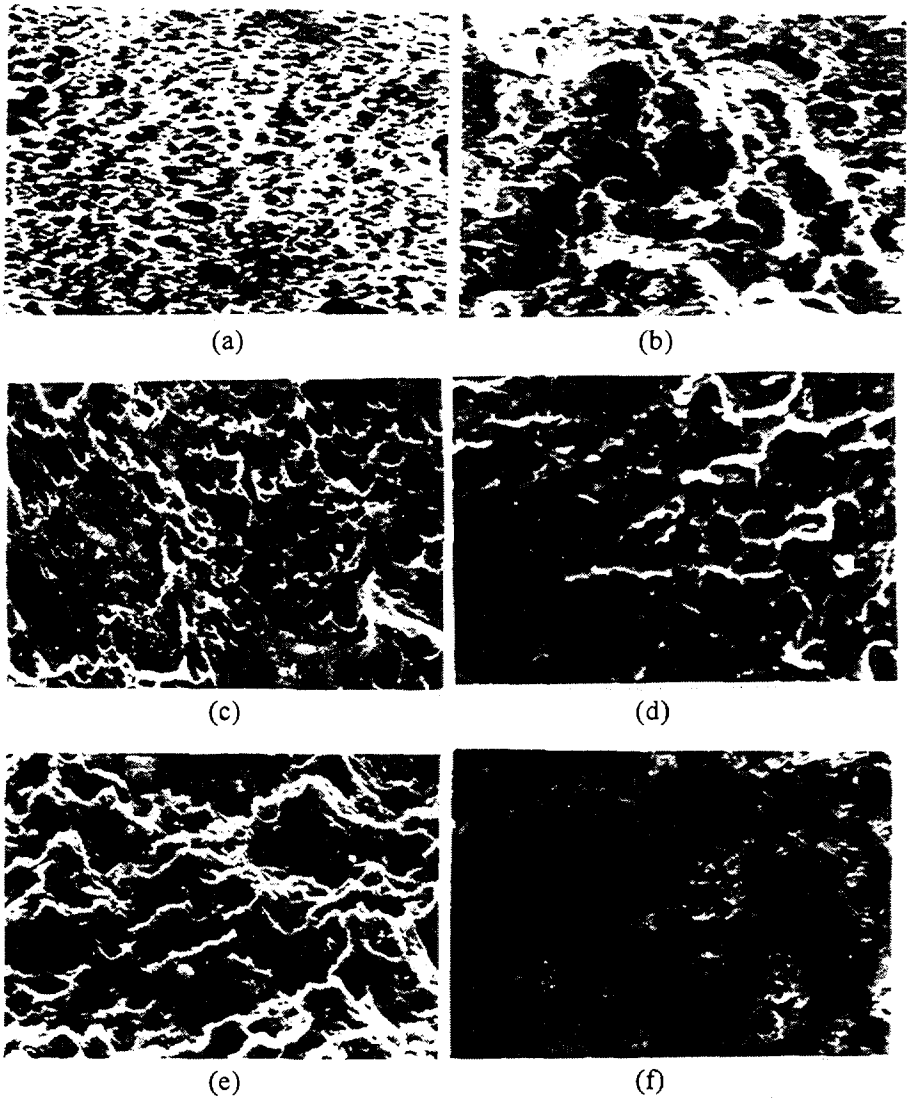

FIG.6 Appearances of fracture for the cladding tube
(a)original cladding tube I
(b)attacked cladding tube I under lower oxygen potential
(c)original cladding tube II
(d)annealed cladding tube II
(e)attacked cladding tube II under lower oxygen potential
(f)attacked cladding tube II under high oxygen potential

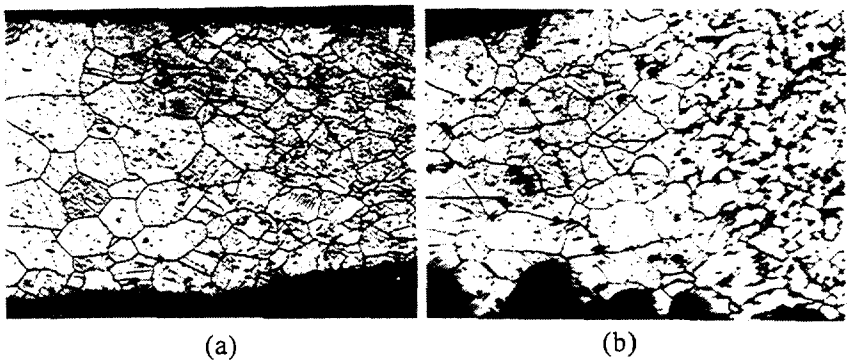

FIG.7 Axial section of the bursted cladding tube II
(a)attacked under lower oxygen potential
(b)attacked under high oxygen potential

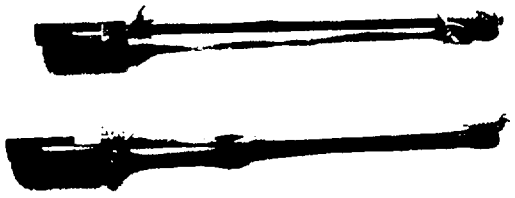

FIG.8 Bursted cladding tubes

TABLE 2 BURST STRENGTH AND CIRCULAR EXPANSION OF 316-TI CLADDING TUBES(1)

Specimens class		Burst strength(MPa)		Circular expansion(%)	
		single	average	single	average
cladding tube I	15%c.w.	685.1		24.67	
		684.8	684.9	29.87	28.14
		684.7		29.89	
	attacked under tested conditions with Cr/Cr_2O_3	—		—	
		673.9	65.17	24.15	25.64
		629.4		27.12	
	attacked under tested conditions with Ni/NiO	breack down before the burst test completion			
cladding tube II	30%c.w.	975.0		6.42	
		975.0	975.0	6.16	6.33
		975.0		6.42	
	above conditions +700℃ annealing 120h	637.0		—	
		715.0	684.7	14.12	16.78
		702.0		19.43	
	attacked nder tested conditions with Cr/Cr_2O_3	669.5		12.26	
		682.5	697.7	16.77	14.52
		741.0		—	
	attacked under tested conditions with Ni/NiO	breack down before the burst test completion			

(1)At room temperature

3.3 Inhibition effectiveness of the oxygen absorbers in the inner wall attack of the cladding tubes

It is well known that the oxygen activity in the gap between cladding and fuel pellet is a very important factor for inner wall attack of the cladding tube at high burnup. With increasing of oxygen potential, the attack on cladding tube inner wall becomes severe. There are two ways to reduce the oxygen activity[20], one is to reduce the initial O/M ratio of the fuel, another is adding of the oxygen absorber in the pin. Lower O/M ratio may lead to decreasing of the thermoconductivity of fuel pellets and increasing the melting probability of the pellets, so adding of the oxygen absorber should be an effective method.

Based on the mechanism of FCCI, Cr, Zr and Nb were selected as the inhibitor respectivery in this investigation. The attack morphologies and depth, the penetration depth of the fission products in the inner surface of the cladding tubes were detected.

3.3.1 Attack morphologies and depth

The attack morphologies of the cladding tubes containing Cr, Zr and Nb are respectively shown in Fig.9(a)—(c). There is severe erosion on the inner surface of the cladding tubes without

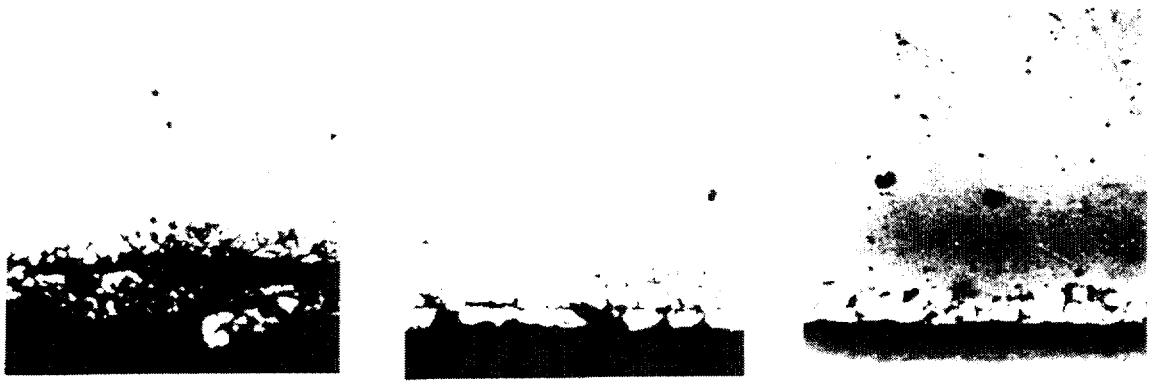

(a) (b) (c)

FIG.9 Inner wall morphologies of the cladding tube II attacked under high oxygen potential
(a)with inhibiter Cr (b)with inhibiter Zr (c)with inhibiter Nb

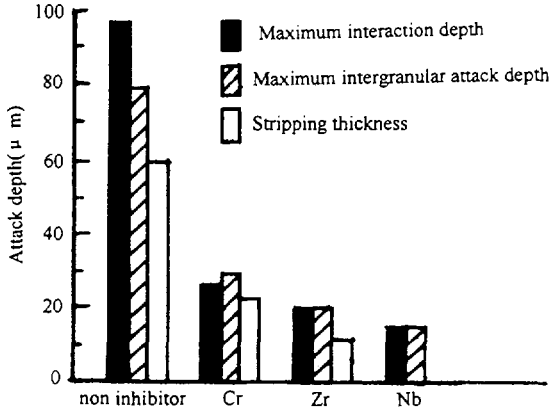

FIG.10 Inner wall attack depth of cladding tube II with and without inhibitor

inhibitor (see Fig.3 (b)). For the cladding tubes with Cr inhibitor, there is also IGA and erosion (Fig.9 (a)), but the depth is more less than that without inhibitor. For the cladding tubes containing inhibitor Zr, a little erosion was observed, the attack depth is less than that with inhibiltor Cr (Fig.9 (b)). Neither erosion nor grain stripping (Fig.9 (c)) was observed, but a little IGA was only observed for the cladding tubes with inhibitor Nb. The inner wall attack depth of the cladding tubes with and without inhibitor is shown in Fig.10.

3.3.2 Fission products penetration

The tellurium penetration along the grain boundary of the cladding inner wall was detected by EPMA and EDAX, and the results are shown in Fig.11 and Fig.12. It is clear that the Te penetration depth and its content reduce orderly with adding of Cr, Zr, Nb inhibitor respectively (Fig.11). EDAX diagram (Fig.12) shows that the peaks of Cr and Te are reduced orderly with adding of Cr, Zr, Nb respectively, and almost no tellurium was detected in the attack area of the cladding inner surface containing inhibitor Nb. A little cesium was detected by EDAX in the grain boundaries of the attacked area for the cladding tubes which containing Cr, Zr and Nb respectively. On the other hand, in the presence of inhibitor Cr, the Cr content in attacked area increases obviously, and in the presence of the inhibitor of Zr and Nb, Zr and Nb were found by EPMA separatly in attacked grain boundaries (table 3). It can be inferred from table 3 and table 4[21,22] that the oxygen reacts with inhibitor in the cladding tubes at first, to form the Cr_2O_3, ZrO_2 and Nb_2O_5 respectively, at the meantime, Cs_xCrO_4 and some Cs-Zr-O and Cs-Nb-O compounds may formed in the attacked grain boundaries, then the surplus oxygen participats the attack of fission products to cladding tubes.

Mereover, with oxygen absorber is loaded into cladding tubes, oxygen activity is descreased, and the stability of cecium compounds (such as Cs_2Te) increased. In this case, the activity of tellurium is dropped, and the attack of Te to the grain bounderies of cladding is decreased.

TABLE 3 THE CONTENTS OF Cr,Zr AND Nb IN ATTACK GRAIN BOUNDARIES

Oxygen absorber	Contert(%)		
	Cr	Zr	Nb
Cr	23.2111	0.0000	—
Zr	19.5908	0.6623	—
Nb	18.2353	0.0000	0.1695

TABLE 4 THE STANDARD FREE ENTHALPY FOR FORMATION OF Cr_2O_3,Zr_2O_2 and Nb_2O_5

Oxide	$\Delta G_{298}K$(kJ • mol^{-1})	$\Delta G_{973}K$(kJ • mol^{-1})
$Cr_2O_3$①	-695.18	-578.26
$ZrO_2$②	-1016.12	-891.87
$Nb_2O_5$③	-1751.95	-1475.33
Cs_2O		-310④

①ΔG_T^O=-746800+173.2 • T(J • mol^{-1})[21]

②ΔG_T^O=-1071000+184.1 • T(J • mol^{-1})[21]

③ΔG_T^O=-446200+97.56 • T(cal • mol^{-1})[22]

④at 1000K[9]

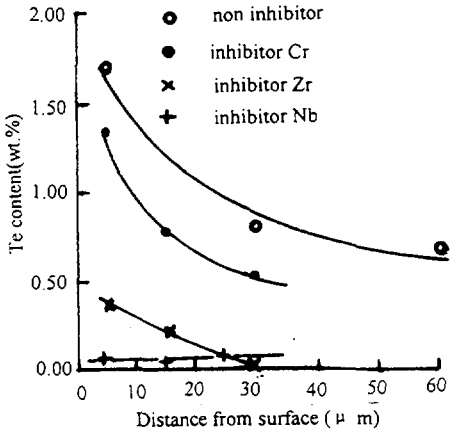

FIG.11 Te penetration in attacked grain boundaries of cladding II

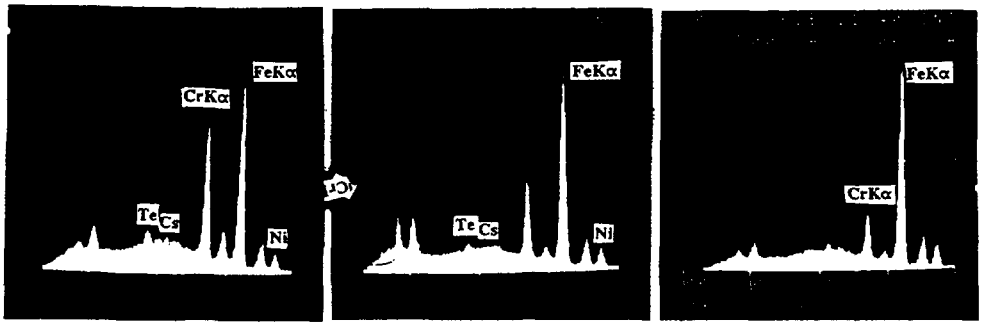

Cr Zr Nb

FIG.12 EDAX diagram in attacked area of cladding tube II

4.CONCLUSION

(1)For the 316-Ti S.S. cladding tubes attacked by fission products Cs, Te, I and Se at 10at.% burnup and 700℃, the shallow intergranular attack or a negligible corrosion under lower oxyen potential with Cr/Cr_2O_3 buffer and the serious erosive attack under high oxygen potential with Ni/NiO buffer were observed. The attack depth for the former is less than 28 μ m, but about 100 μ m is for the later.

(2)The degradations of strength and toughness for attacked tubes under high oxygen potential are considerably larger than that under lower oxygen potential. The appearance of fracture is intergranular brittle for the attacked cladding tubes under high oxygen potential, while the tenacious under lower oxygen potential.

(3)The oxygen absorbers inhibit significantely the inner wall attack of 316-Ti S.S. cladding tubes with the order of the inhibition effectiveness Nb>Zr>Cr. The niobium may become an effective inhibitor for the erosive and intergranular attack of fission products to FBR fuel pin cladding at high burnup.

REFERENCES

[1] O.Götzman, P.Hofman and F.thummler
J.Nucl.Mater.52(1974)33

[2] L.A.Lawrence and J.W.Jost
Trans. Am. Nucl. Soc. 36(1981)211

[3] L.A.Lawrence
Trans. Am. Nucl. Soc, 32,(1979)249

[4] M.G.Adamson, E.A.Aitken,S.K.Evans,W.Mccarthy
US GEAP-14075 (Dec.1976)

[5] M.G.Adamson
Technical Committee Meeting On Fule And Cladding Interaction
IWGFR-16,Tokyo,Japan.1977. p180

[6] M.G.Adamson
Technical Committee Meeting On Fule And Cladding Interaction
IWGFR-16, Tokyo,Japan.1977. p108

[7] M.G.Bradury, S.Pickering, W.H.Whitiow
Technical Committee Meeting On Fule And Cladding Interaction
IWGFR-16, Tokyo,Japan.1977.p51

[8] O.Götzmann
Report of Int. Conf. On Fast Reactor core And Fuel Structural Behaviour
(BNES, London,1990)

[9] C.T.Walker, S.Pickering
Nucl. Technol.42-43(1979)207

[10] M.G.Adamson,E.A.Aitken
J.Nucl.Mater.132(1985)160

[11] O.Götzmann
Technical Committee Meeting On Fule And Cladding Interaction
IWGFR-16,Tokyo,Japan.1977.p37

[12] L.Schafer,P.Hofmann
J.Nucl.Mater.115(1983)169

[13] O.Götzmunn, O.Hofmann
J.Nucl.Mater.59—60(1976)194

[14] M.Koizumi,H.Furuya, S.Nagai,H.Kawamata
Technical Committee Meeting On Fule And Cladding Interaction
IWGFR-16,Tokyo,Japan.1977.p73

[15] D.R.Duncan,N.F.Panayotou,E.L.Wood
Trans.Am.Nucl.Soc.38(1981)265.

[16] C.W.Hunten,G.D.Johnson
Int. Conf.On Fast Breeder Reactor Fuel Performance ANS.Monterey, California, 1979. p478
[17] S.Vaidyanathan,M.G.Admson
Trans.Am.Nucl.Soc.38(1981)262
[18] M.G.Adamson
Metal Trans.17A(1986)2090
[19] J.A.Hemsworth,M.G.Nicholas, R.M.Crispin
J.Mater.Sci.25(1990)5248
[20] E.T.Weber,L.A.Lawrenc and C.N.Wilson(HEDL),M.G.Adamson(GE)
Proc.Int.Conf. Fast Breeder Reactor,Monterey California,1979.p445
[21] Cheng Lanzheng,Zhang Yanhao
《Physics and Chemistry》 by Shanghai Science Techology Press,Appendix III,1988
[22] Yei Tianlun
《Metallurgy Thermodynamical》 Zhongnan Engineering College press,Appendix9, 1987